
Experiment 1: Uniform Acceleration

Samiha Rahman

UID: 404792929

Date of Experiment: August 14, 2017

Lab Section: Monday/Wednesday,
11:30 AM

TA: Nicholas Rombes III

Lab Partner: Rafi Hessami,
Ahmad Al Shareef

WORKSHEET

I. Plot

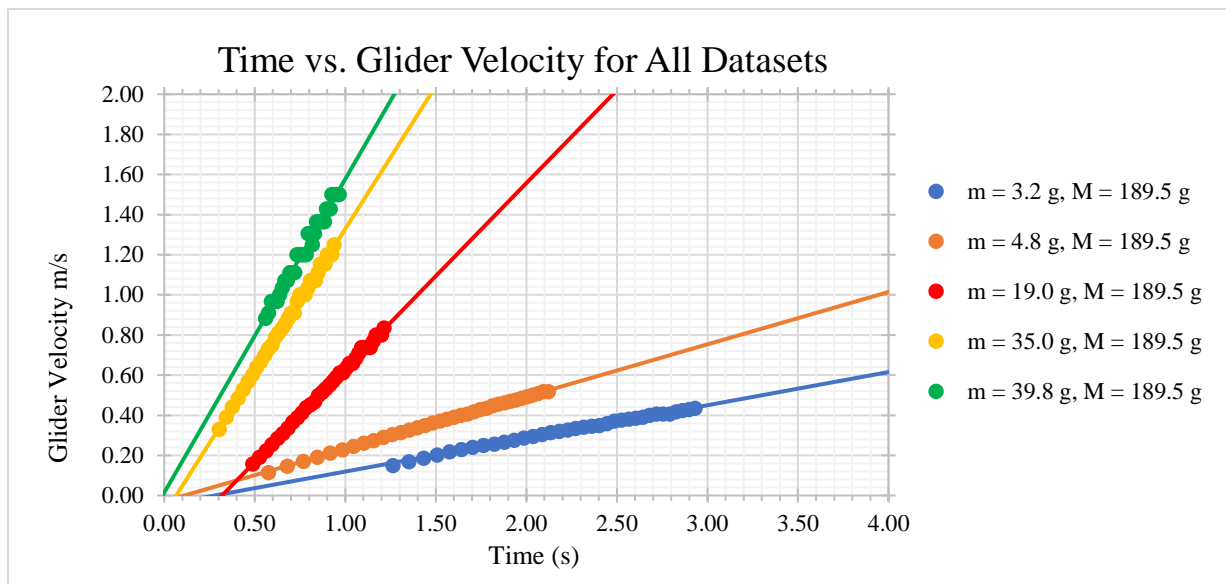


Figure 1. Average Velocity vs. Time for all five glider-mass pulley systems. For $m = 3.2 \text{ g}, M = 189.5 \text{ g}$ the fit equation is $v(t) = (0.161 \pm 0.003)t \frac{m}{s^2} + (0.111 \pm 0.004) \frac{m}{s}$. For $m = 4.8 \text{ g}, M = 189.5 \text{ g}$, the fit equation is $v(t) = (0.238 \pm 0.003)t \frac{m}{s^2} - (0.041 \pm 0.005) \frac{m}{s}$. For $m = 19.0 \text{ g}, M = 189.5 \text{ g}$, the fit equation is $v(t) = (0.886 \pm 0.006)t \frac{m}{s^2} + (0.275 \pm 0.003) \frac{m}{s}$. For $m = 35.0 \text{ g}, M = 189.5 \text{ g}$, the fit equation is $v(t) = (1.42 \pm 0.01)t \frac{m}{s^2} - (0.094 \pm 0.008) \frac{m}{s}$. For $m = 39.8 \text{ g}, M = 189.5 \text{ g}$, the fit equation is $v(t) = (1.56 \pm 0.03)t \frac{m}{s^2} + (0.01 \pm 0.03) \frac{m}{s}$. Since only the slope is of concern, the intercepts are ignored.

II. Data Table

Trial	Hanging mass $m_{\text{best}} \text{ (g)}$	Glider mass $M_{\text{best}} \text{ (g)}$	Fit acceleration $a_{\text{fit}} \text{ (m/s}^2\text{)}$	Predicted acceleration $a_{\text{fit}} \text{ (m/s}^2\text{)}$
1	3.2	189.5	0.161 ± 0.003	0.163 ± 0.003
2	4.8	189.5	0.238 ± 0.003	0.242 ± 0.003
3	19	189.5	0.886 ± 0.006	0.893 ± 0.002
4	35	189.5	1.42 ± 0.01	1.528 ± 0.002
5	39.8	189.5	1.56 ± 0.03	1.701 ± 0.002

Table 1. Masses, Fit and Predicted Acceleration for Each Dataset

III. Derivations

Derivation of Equation 1.1 (acceleration of system)

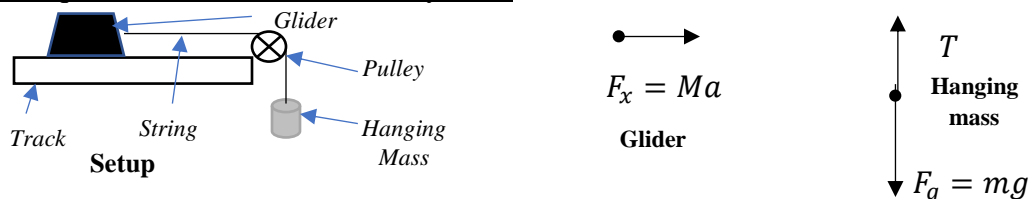


Figure 2. Set-up of the track, glider, mass, and pulley system. Simplified diagram on the left and corresponding free body diagrams for the glider and hanging mass on the right.

Based on Figure 2, we can assume that $T = F_x$. We also know that a represents the acceleration of the entire system, which is also equivalent to the acceleration of either the hanging mass or glider as well. Along with Newton's second law for the hanging mass, we thus yield the following system of equations:

$$\begin{aligned} F_g &= mg \\ T &= F_x = Ma \\ \Sigma F &= (F_g - T) = ma \end{aligned}$$

We substitute F_g and T with their equivalent expressions and solve:

$$\begin{aligned} mg - Ma &= ma \\ gm &= ma + Ma = a(m + M) \end{aligned}$$

Therefore, by dividing we yield equation 1.1,

$$a = \frac{gm}{m + M}$$

Propagations of Uncertainties for Predicted Acceleration

The above formula for calculating predicted acceleration has three operations in the following order: multiplication by an exact number, addition, and division. Each of these operations yield an uncertainty that is carried on to the final step; to find these uncertainties, we make use of the formulas from section ii.2.1 in the lab manual:

The measurements used are (we assume m and M are expressed in kilograms)

$$\begin{aligned} m &= m_{best} \pm \delta m \\ M &= M_{best} \pm \delta M \end{aligned}$$

To compute the uncertainty for $f = gm$, equation ii.21 from the manual is used:

$$\begin{aligned} \delta f &= |A| \delta x \\ \delta(gm) &= |g| \delta m \end{aligned}$$

To compute the uncertainty for $u = m + M$, use equation ii.22

$$\begin{aligned} \delta u &= \sqrt{(\delta x)^2 + (\delta y)^2 + (\delta z)^2 + \dots} \\ \delta(m + M) &= \sqrt{(\delta m)^2 + (\delta M)^2} \end{aligned}$$

The final operation thus is $u = a = \frac{f_{best} \pm \delta f}{u_{best} \pm \delta u}$, and equation ii.23

$$\begin{aligned} \delta u &= u_{best} \sqrt{\left(\frac{\delta x}{x_{best}}\right)^2 + \left(\frac{\delta y}{y_{best}}\right)^2 + \dots} \\ \delta a &= \frac{|f_{best}|}{|u_{best}|} \sqrt{\left(\frac{\delta f}{f_{best}}\right)^2 + \left(\frac{\delta u}{u_{best}}\right)^2} \end{aligned}$$

Substituting in the appropriate equivalent expressions yields:

$$\delta a = \frac{g(m_{best})}{m_{best} + M_{best}} \sqrt{\left(\frac{|g|\delta m}{g(m_{best})}\right)^2 + \left(\frac{\sqrt{(\delta m)^2 + (\delta M)^2}}{m_{best} + M_{best}}\right)^2}$$

This single formula can be used to calculate δa for each dataset. The uncertainties of m and M are $\delta m = 0.00005 \text{ kg}$ and $\delta M = 0.0001 \text{ kg}$, the latter being due to the addition of masses. The calculations have been done by substituting in the corresponding m_{best} , δm , M_{best} and δM values and can be referred to in Table 1.

IV. Conclusions

As can be observed in Table 1, the fitted acceleration is a bit lower than the predicted acceleration for each system. This was however expected due to the conscious neglect of friction and drag. Friction and air resistance cannot be realistically eliminated in the environment of our lab. Therefore, the friction between the glider and track as well as between the string and pulley decreased acceleration. The experiment can be improved by using lubricated equipment or more advanced equipment made of such material that minimizes friction even more. To decrease drag, the environment can be controlled to have a lower air density.

An issue regarding the larger masses is that it is possible that the string often slipped due to the high acceleration; this high acceleration of the string was thus not reflected onto the turning pulley, leading to lower values for the last two trials. The main way this can be reduced while maintaining the current mass limits is using sturdier string and bigger pulley (these however increase friction so is a condition improvement).

Another potential source of error is error from the devices used. If taring does not solve the issue of accuracy, more advanced and accurate equipment is the main solution to fixing this issue.

While all the above most likely affected the measured values, the experiment nonetheless concluded the expected relationship that increasing mass of the hanging object would increase the acceleration of the system.

V. Extra Credit

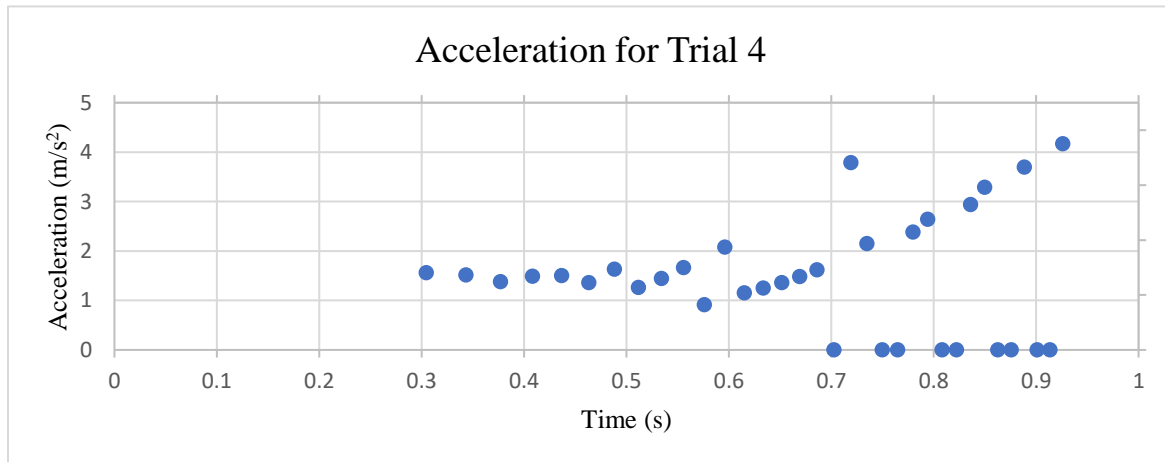


Figure 2. Acceleration vs. Time for $m = 35.0 \text{ g}$, $M = 189.5 \text{ g}$. The average acceleration was found between each (time, velocity) point by dividing change in velocity over change in time for every two points.

As can be observed in Figure 2, after a certain point during the run, there is a lot of noise. The data points past $t = 0.7$ seconds seem to alternate between 0 m/s^2 and $>2.0 \text{ m/s}^2$, which are values far from the true value. This indicates that the pulley was sometimes rotating at a constant velocity and then suddenly increasing in velocity; such behavior implies that the string often slipped, causing the acceleration to increase temporarily. However, when the string temporarily lost contact with the pulley, the increasing velocity of the string did not project onto the pulley; this led to a projection of 0 m/s^2 . This in effect led to quite a bit of noise.

The mean of all these values is $a_{avg} = (1.46 \pm 0.20) \text{ m/s}^2$. The mean was found using the AVERAGE() function in Excel and the formula for statistical uncertainty δa is $\delta a =$

$$\frac{1}{\sqrt{N}} \sqrt{\frac{1}{N-1} \sum_{i=1}^N (x_i - \bar{x})^2} = \frac{\sigma_x}{\sqrt{N}} \text{ (from equation ii.23 in the lab manual); this was found using the}$$

equation STDEV.S()/N (where $N = 34$). On the contrary, the fitted equation for Trial 4 is $a_{fitted} = (1.42 \pm 0.01) \frac{\text{m}}{\text{s}^2}$. While numerically, the method of calculating acceleration values yielded a result that included the true value, it is not a very reliable method. The main reason the true value is included is due to the high uncertainty of mean value. The method of using the slope of a fitted time vs velocity plot is somewhat inaccurate but is nonetheless precise. On the other hand, the latter method is not precise, which is why it included an accurate value. Due to this lack of precision, it is doubtful that such accuracy can be met every time, especially when the “best” value is almost as inaccurate as that of the fitted slope value. The linear regression method is thus a more reliable measure of the acceleration.

PRESENTATION MINI-REPORT

The theory of cochlear mechanics has been actively developing for the past 200 years. The process of how sound is analyzed in the cochlea, the inner ear cavity, was initially answered by Hermann von Helmholtz in 1850. Helmholtz theorized that the cochlea breaks down sound and determines its frequencies through resonance. This resonance theory was however contradicted a century later by Georg von Békésy who deemed impossible the resonance of such microscopic components, which are immersed in cochlear fluid¹. In place of this, he observed travelling waves in human bones, thus concluding that instead the basilar membrane on the cochlea is responsible for sending a response to a sound vibration. For each frequency component of the sound, the membrane produces a traveling wave”². With anomalies contradicting either or both theories, observation done since the development of both these theories tend towards using the latter theory as the base of their research. Nonetheless, the merit of both theories has embedded both as the foundation for the ongoing exploration of cochlear mechanics today¹.

The current focus of cochlear mechanics has been motivated by the development of cochlear implants. While such technology has advanced immensely and satisfies individuals suffering from hearing loss, the device cannot be perfected until the complete structure and processes of the cochlea can be understood and replicated. The analysis and observation thus investigates the process of the cochlear amplifier. The behavior of the cochlear amplifier is likened to a precise resonator of high quality. The system is defined as an “active” process as

opposed to the passive travelling waves from the basilar membrane³. The passive system of travelling waves and active system of the cochlear amplifier combine to capture the dynamic range of human hearing. Both nonlinear, they compress this range into a smaller range comprised of the movement of hair cells³. These hair cells are situated on a strip on the basilar membrane. This strip—known as the organ of Corti—holds these mechanosensitive hair cells whose reaction to the sound vibrations are translated into neural signals that communicate with the brain³.

With the knowledge of these highly sensitive hair cells, cochlear implants have been developed to aide a hearing loss patient by combining electric and acoustic stimulation of the cochlea. This allows for low frequency hearing such as localized sound and music while also giving access to high frequency sounds. The issue however is that cochlear implantation often leads to the loss of a patient's residual hearing. The preservation of this hearing is necessary to provide acoustic hearing; otherwise the benefits of the combined stimulation cannot be reaped⁴.

Fortunately, recent studies have identified a connexin30 mutation that preserves hearing. Connexin30, a gap junction protein that contributes to the energy distribution that leads to cochlear amplification, is encoded by the GJB6 gene. While mutations of this gene generally are what lead to hearing loss diseases, a p.Ala88Val (A88V) mutation in the gene actually protects a part of the basal membrane of adults. This leads to a rescue of hearing⁵, something that cochlear implantation often makes worse. In addition, the observation of this mutation in adult mice has provided more information on the actual roles of the gap junction proteins in cochlear amplification⁵. Based on this discovery, the future of cochlear implants will mostly likely implement the results of further analysis of this mutation. Information on the resulting structure due to this mutation can be used to create a cochlear implant that can preserve the residual hearing during the risky insertion of the device. This will likely achieve benefits of the combined-simulation cochlear implant, allowing hearing loss patients to once again use their ears to their full potential.

Word Count: 609

References

1. Bell, A. A Resonance Approach to Cochlear Mechanics. *Public Library of Science ONE*, **7**, 11 (2012).
2. Davis, H. An active process in cochlear mechanics. *Hearing Research*, **9**, 1, 79-90 (1983).
3. Reichenbach T, Hudspeth A.J. The physics of hearing: fluid mechanics and the active process of the inner ear. *Progress in Physics*, **77**, 7 (2014).
4. Greene, Nathaniel T. *et al.* Cochlear Implant Electrode Effect on Sound Energy Transfer within the Cochlea during Acoustic Stimulation. *Otology & neurotology: official publication of the American Otological Society, American Neurotology Society [and] European Academy of Otology and Neurotology*, **37**, 1554–1561 (2015).
5. Lukashkina, V. A. *et al.* A connexin30 mutation rescues hearing and reveals roles for gap junctions in cochlear amplification and micromechanics. *Nature Communications*, **8**, 14530 (2017).